Biswajit Bera / International Journal of Engineering Research and Applications (IJERA)
ISSN: 2248-9622 www.ijera.com
Vol. 2, Issue 5, September- October 2012, pp.404-411

# Adhesional Friction Law and Adhesive Wear Law of Micromechanical Surface Contact

**Biswajit Bera***
*(Department of Mechanical Engineering, National Institute of Technology Durgapur, India)

## ABSTRACT

**The paper describes the investigation on adhesional friction law and adhesive wear law of micromechanical surface contact. Adhesion theory of loading force and friction force is incorporated in multiasperity contact to find out static coefficient of friction which supports Amontons's law of friction. New adhesive wear law is developed from almost linear relationship of dimensionless real area of contact and dimensionless adhesive wear volume, and it is compared with existing Archard's adhesive wear law.**

*Keywords* - **Real area of contact, Adhesional loading force, Adhesional friction force, Coefficient of friction, Adhesive wear law**

## 1. Introduction

Friction could be defined as the force of resistance that occurs when one body moves tangentially over another body. In the 15th century da Vinci discovered a law about dry sliding friction, which was rediscovered by Amontons about 200 years later. Friction laws were stated by French engineer Guillaume Amontons [1] in 1699 from the conclusions of his experimental work which are given as follows:

a) The friction force linearly proportional to the normal load between the two bodies in contact.
b) The friction force is independent of the apparent area of contact between the two bodies.

Thereafter, microscopic analysis of friction process was described by Bowden and Tabor [2] in 1931. The theory was based on following two statements:

a) The friction force is dependent on real area of contact between two bodies.
b) The friction force is dependent on shearing strength of adhesive bond formed between two bodies at tip of asperities.

The adhesional friction theory of Bowden and Tabor is appeared to be inconsistent with Hertz theory of deformation of contacting elastic asperities, which predicts that the contact area should vary as 2/3 power of load $\left(P=\frac{Ka^3}{R}\Rightarrow \pi a^2 \propto P^{2/3}\right)$.To avoid the violation of the theory, Bowden and Tabor simply, mentioned that all asperities should deform plastically and real area of contact is linearly proportion to load $\left(P=\pi a^2 H \Rightarrow \pi a^2 \propto P\right)$. Though the theory is well accepted, still there is a question why real area of contact is linearly proportional to load in so many tribosystem where plastic deformation does not occur.

This is investigated in adhesive MEMS surface contact considering adhesion model of elastic solid. However, there are two type of adhesion model of elastic solid; one is JKR adhesion model [3] which considers adhesion force within contact area of elastics solid sphere and another is DMT adhesion model [4] which considers adhesive force out side of contact area of elastic solid sphere. First of all, Chang et al. [5] have developed multiasperity adhesion model of metallic rough surface contact based on DMT adhesion model. Thereafter, Roychowdhury and Gosh [6] have considered JKR adhesion model for study of adhesive rough surface contact but have evaluated external Hertzian load in presence of adhesion, though which could be evaluated directly. However, adhesion component of JKR model is not considered for evaluation of adhesion of multiasperity rough surface contact. The adhesive component of JKR adhesion model is considered for present study of adhesive MEMS surface contact. Actually, Johnson et al. [3] has extended Hertz model considering adhesion of solid elastic sphere based on energy method. Thereafter, on the basis of same method, Savkoor and Briggs [7] has extended JKR adhesion model and developed adhesional friction model of elastic solid sphere under tangential loading. The SB adhesional friction model is considered for finding adhesional friction of MEMS surface contact.

On the other hand, due to rapid growth of micro-machine, it has become important to study the wear phenomena in the nano-scale under ultra low loading condition. Archard's adhesive wear law [11] is essentially based on the classical concept of adhesion of metallic surface as proposed by Bowden and Tabor [2]. The fundamental idea is that the welded junctions are formed at the pick of the

asperities due to localized high adhesion and the subsequent shearing of the junctions from weaker material causing adhesive wear. Similar idea is implemented to find new adhesive wear law considering adhesion component of JKR adhesion model [3]. Thereafter, it is compared with existing Archard's adhesive wear law.

## 2. Single asperity contact

### 2.1 Single asperity real area of contact

JKR adhesion theory has modified Hertz theory of spherical contact. It predicts a contact radius at light loads greater than the calculated Hertz radius. As asperity tip is considered spherical, the adhesion model of single asperity contact could be extended to multiasperity of rough surface contact. So, real contact area of single asperity is

$$A_a = \pi\left[\frac{R}{K}\left(F_0 + 3\pi\gamma R + \sqrt{6\pi\gamma RF_0 + (3\pi\gamma R)^2}\right)\right]^{\frac{2}{3}}$$

Substituting $F_a = \frac{K(R\delta)^{1.5}}{R}$, we get

$$A_a = \pi\left[R^{1.5}\delta^{1.5} + \frac{3\pi\gamma R^2}{K} + \sqrt{\frac{6\pi\gamma R^{3.5}\delta^{1.5}}{K} + \frac{9\pi^2\gamma^2R^4}{K^2}}\right]^{\frac{2}{3}} \quad (1)$$

### 2.2 Single asperity adhesional loading force

According to JKR adhesion model, the expression of adhesional loading force for each asperity contact is

$$F_a = F_0 + 3\pi\gamma R + \sqrt{6\pi\gamma RF_0 + (3\pi\gamma R)^2}$$

$$= KR^{0.5}\delta^{1.5} + 3\pi\gamma R + \sqrt{6\pi\gamma KR^{1.5}\delta^{1.5} + (3\pi\gamma R)^2} \quad (2)$$

where $\frac{1}{K} = \frac{3}{4}\left(\frac{1-\nu_1^2}{E_1} + \frac{1-\nu_2^2}{E_2}\right)$

and $E_1$, $E_2$, $\nu_1$ and $\nu_2$ are Young's modulus and poisson's ratios of the contacting surfaces respectively,

where surface energy of both surfaces, $\gamma = \gamma_1 + \gamma_2 - \gamma_{12}$

### 2.3 Single asperity adhesional friction force

Savkoor and Briggs theory has found adhesional friction of spherical contact under tangential loading. As asperity tip is considered spherical, the adhesional friction model of single asperity contact could be extended to multiasperity of rough surface contact. According to the Savkoor and Briggs model, the expression of adhesional friction force for each asperity contact is

$$T_a = \frac{4}{\sqrt{\left(K/G\right)}}\sqrt{\left(2\pi\gamma RF_0 + 3(\pi\gamma R)^2\right)}$$

$$= \frac{4}{\sqrt{\left(K/G\right)}}\sqrt{\left(2\pi\gamma KR^{1.5}\delta^{1.5} + 3(\pi\gamma R)^2\right)} \quad (3)$$

where $\frac{1}{G} = \frac{2-\nu_1}{G_1} + \frac{1-\nu_2}{G_2}$

### 2.4 Single asperity adhesive wear volume

If wear particle is in the shape of hemispherical and is cut off from tip of the asperity, wear volume is

$$V_a = \frac{2}{3}\pi a^3$$

$$= \frac{2}{3}\pi\left[\frac{R}{K}\left(F_0 + 3\pi\gamma R + \sqrt{6\pi\gamma RF_0 + (3\pi\gamma R)^2}\right)\right]$$

Substituating $F_0 = \frac{K(R\delta)^{1.5}}{R}$, we get

$$V_a = \frac{2}{3}\pi\left[R^{1.5}\delta^{1.5} + \frac{3\pi\gamma R^2}{K} + \sqrt{\frac{6\pi\gamma R^{3.5}\delta^{1.5}}{K} + \frac{9\pi^2\gamma^2R^4}{K^2}}\right] \quad (4)$$

## 3. Multiasperity contact

First of all, Greenwood and Williamson [8] developed statistical multyasperity contact model of rough surface under very low loading condition and it was assumed that asperities are deformed elastically according Hertz theory. Same model is modified here in adhesive rough surface contact and it is based on following assumptions:

i. The rough surface is isotropic.
ii. Asperities are spherical near their summits.
iii. All asperity summits have the same radius R but their heights vary randomly.
iv. Asperities are far apart and there is no interaction between them.
v. Asperities are deform elastically according to JKR adhesion theory
vi. There is no bulk deformation. Only, the asperities deform during contact.

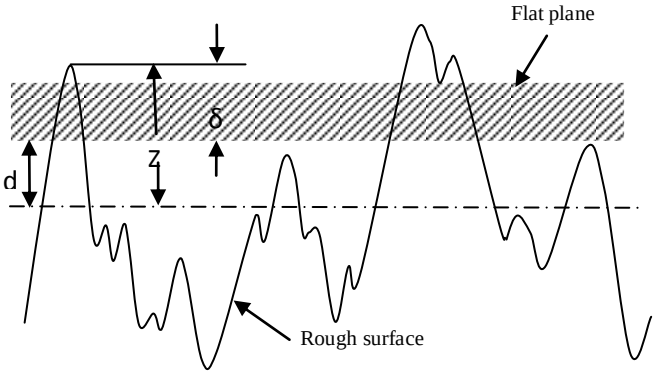


Fig. 1 Rough surfaces contact

Multiasperity contact of adhesive rough surface has shown in Fig.1. According to, GW model, two rough surface contact could be considered equivalently, contact between rough surface and smooth rigid surface. Let z and d represents the asperity height and separation of the surfaces respectively, measured from the reference plane defined by the mean of the asperity height. δ denotes deformation of asperity by flat surface. Number of asperity contact is

$$N_c = N\int_d^\infty \phi(z)dz \qquad (5)$$

where *N* is total number of asperity and $\phi(z)$ is the Gaussian asperity height distribution function.

3.1 Multiasperity real area of contact

So, from eq$^n$ (1) and (5), real area of contact for multiasperity contact is

$$A = N\int_d^\infty A_a\phi(z)dz$$

$$= N\int_d^\infty \pi\left[R^{1.5}\delta^{1.5} + \frac{3\pi\gamma R^2}{K} + \sqrt{\frac{6\pi\gamma R^{3.5}\delta^{1.5}}{K} + \frac{9\pi^2\gamma^2R^4}{K^2}}\right]^{\frac{2}{3}}\phi(z)dz$$

Dividing both side by apparent area of contact $A_n$

$$A^* = \int_0^\infty \left[\frac{\pi^{1.5}(\eta R\sigma)^{1.5}\Delta^{1.5} + 3\pi^{2.5}(\eta R\sigma)^{1.5}\left(\frac{\gamma}{K\sigma}\right)\left(\frac{R}{\sigma}\right)^{0.5} + \sqrt{6\pi^4(\eta R\sigma)^3\left(\frac{\gamma}{K\sigma}\right)\left(\frac{R}{\sigma}\right)^{0.5}\Delta^{1.5} + 9\pi^5(\eta R\sigma)^3\left(\frac{\gamma}{K\sigma}\right)^2\left(\frac{R}{\sigma}\right)}}\right]\phi(\Delta)d\Delta$$

$$= \int_0^\infty \left[\frac{\pi^{1.5}A_0^{1.5}\Delta^{1.5} + 3\pi^{2.5}A_0^{1.5}B_0R_0^{0.5} + \sqrt{6\pi^4A_0^3B_0R_0^{0.5}\Delta^{1.5} + 9\pi^5A_0^3B_0^2R_0}}\right]\frac{1}{\sqrt{2\pi}}\exp\left[-\frac{(h+\Delta)^2}{2}\right]d\Delta$$

3.2 Multiasperity adhesional loading force

So, , from eq$^n$ (2) and (5), adhesional loading force for multiasperity contact is

$$F = N_cF_a$$

$$= N\int_d^\infty \left[KR^{0.5}\delta^{1.5} + 3\pi\gamma R + \sqrt{6\pi\gamma KR^{1.5}\delta^{1.5} + (3\pi\gamma R)^2}\right]\phi(z)dz$$

Dividing both side by $A_nK$

$$F^* = \int_0^\infty \left[\frac{(\eta R\sigma)\left(\frac{R}{\sigma}\right)^{-0.5} + 3\pi(\eta R\sigma)\left(\frac{\gamma}{K\sigma}\right) + \sqrt{6\pi(\eta R\sigma)^2\left(\frac{\gamma}{K\sigma}\right)\left(\frac{R}{\sigma}\right)^{-0.5}\Delta^{1.5} + 9\pi^2(\eta R\sigma)^2\left(\frac{\gamma}{K\sigma}\right)^2}}\right]\phi(\Delta)d\Delta$$

$$= \int_0^\infty \left[\frac{A_0R_0^{-0.5} + 3\pi A_0B_0 + \sqrt{6\pi A_0^2B_0R_0^{-0.5}\Delta^{1.5} + 9\pi^2A_0^2B_0^2}}\right]\frac{1}{\sqrt{2\pi}}\exp\left[-\frac{(h+\Delta)^2}{2}\right]d\Delta$$

where dimensionless surface roughness parameter, $A_0 = \eta R\sigma$ and dimensionless surface energy parameter, $B_0 = \frac{\gamma}{K\sigma}$

3.3 Multiasperity adhesional friction force

So, , from eq$^n$ (3) and (5), total adhesional friction force for multiasperity contact is

$$T = N_cT_a$$

$$= N\int_d^\infty \left[\frac{4}{\sqrt{\left(K/G\right)}}\sqrt{\left(2\pi\gamma KR^{1.5}\delta^{1.5} + 3(\pi\gamma R)^2\right)}\right]\phi(z)dz$$

Dividing both side by $A_nK$

$$T^* = \int_0^\infty \left[\frac{4}{\sqrt{\left(K/G\right)}}\sqrt{2\pi(\eta R\sigma)^2\left(\frac{\gamma}{K\sigma}\right)\left(\frac{R}{\sigma}\right)^{-0.5}\Delta^{1.5} + 3\pi^2(\eta R\sigma)^2\left(\frac{\gamma}{K\sigma}\right)^2}\right]\phi(\Delta)d\Delta$$

$$= \int_0^\infty \left[\frac{4}{\sqrt{\left(K/G\right)}}\sqrt{2\pi A_0^2B_0R_0^{-0.5}\Delta^{1.5} + 3\pi^2A_0^2B_0^2}\right]\frac{1}{\sqrt{2\pi}}\exp\left[-\frac{(h+\Delta)^2}{2}\right]d\Delta$$

3.4 Multiasperity adhesive wear volume

So, from eq$^n$ (4) and (5), adhesive wear volume for multiasperity contact is

$$V = N_cV_a$$

$$= N\int_d^\infty V_a\phi(z)dz$$

$$= N\int_d^\infty \frac{2}{3}\pi\left[R^{1.5}\delta^{1.5} + \frac{3\pi\gamma R^2}{K} + \sqrt{\frac{6\pi\gamma R^{3.5}\delta^{1.5}}{K} + \frac{9\pi^2\gamma^2R^4}{K^2}}\right]\phi(z)dz$$

Dividing both side by $A_n\sigma$

$$V^* = \frac{2}{3}\pi\int_0^\infty \left[\frac{(\eta R\sigma)\left(\frac{R}{\sigma}\right)^{0.5}\Delta^{1.5} + 3\pi(\eta R\sigma)\left(\frac{\gamma}{K\sigma}\right)\left(\frac{R}{\sigma}\right) + }{\sqrt{6\pi(\eta R\sigma)^2\left(\frac{\gamma}{K\sigma}\right)\left(\frac{R}{\sigma}\right)^{1.5}\Delta^{1.5} + 9\pi^2(\eta R\sigma)^2\left(\frac{\gamma}{K\sigma}\right)^2\left(\frac{R}{\sigma}\right)^2}}\right]\phi(\Delta)d\Delta$$

$$= \frac{2}{3}\pi\int_0^\infty \left[\frac{A_0 R_0^{0.5}\Delta^{1.5} + 3\pi A_0 B_0 R_0 + }{\sqrt{6\pi A_0^2 B_0 R_0^{1.5}\Delta^{1.5} + 9\pi^2 A_0^2 B_0^2 R_0^2}}\right]\frac{1}{\sqrt{2\pi}}\exp\left[-\frac{(h+\Delta)^2}{2}\right]d\Delta$$

## 4. Results and Discussion

Tayebi and Polycarpou [9] have done extensive study on polysilicon MEMS surfaces and four different MEMS surface pairs. Similarly, tribological properties of the MEMS surfaces are being considered for present study as input data as shown in table 1 [Appendix A].The material properties of MEMS surface samples are modulus of elasticity, $K = {}^4/_3 E$ = 112 GPa, modulus of rigidity, G = 18.42 GPa hardness, H = 12.5 GPa, and poisions ratio, $\nu_1 = \nu_2 = 0.22$

### 4.1 Investigation on adhesional friction law

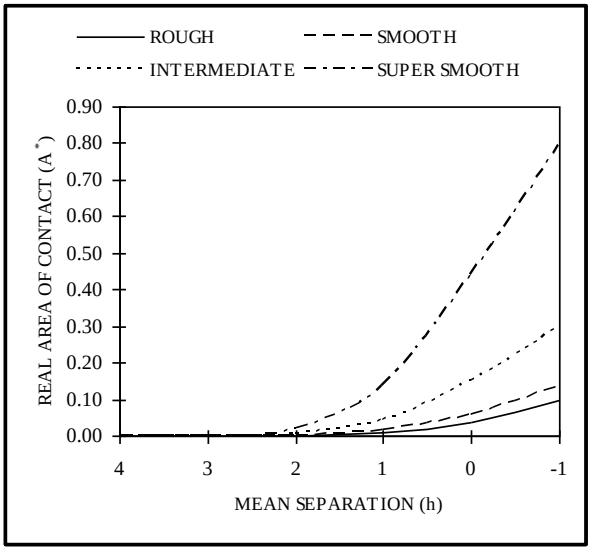


Fig.2 Real area of contact

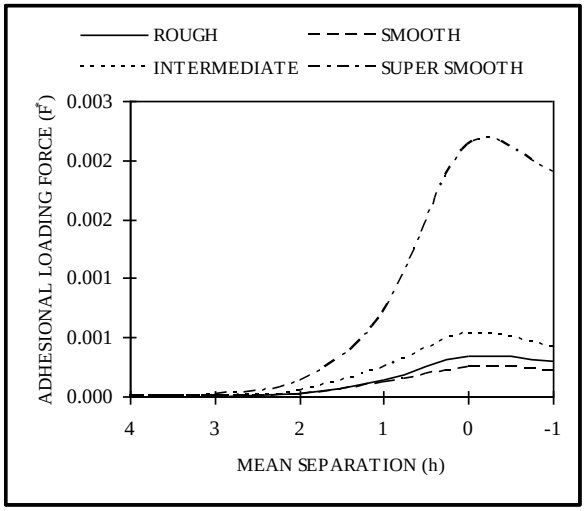


Fig.3 Adhesional loading force

Johnson et. al. first mentioned that deformation of spherical contact would be greater than the deformation predicted by Hertzian spherical contact. It is mentioned that only attractive adhesive force acts within Hertzian contact area and it increases deformation of sphere resulting higher contact area. From Fig.2, dimensionless real area of contact increases with decrement of dimensionless mean separation exponentially. It is found that maximum real areas of contact for the all cases of MEMS surfaces increase as smoothness of MEMS surfaces increase. Dimensionless real area of contact for super smooth MEMS surface is very high almost near to the apparent area of contact due to presence of strong attractive adhesive force. On the other hand, real area of contact is very small for the rough MEMS surface contact. Fig.3 depicts variation of dimensionless adhesional loading force with dimensionless mean separation. From the loading expression of JKR adhesion model, it is found there is two component of force; one is Hertzian deformation force (i.e. external force) and another is adhesive force. Fig.3 shows that adhesional loading forces are also increases with decrement of dimensionless mean separation exponentially. As smoothness of MEMS surfaces increases, deformation force decreases but adhesive force increases. So, deformation force and adhesive force are inversely proportional according to consideration of roughness as well as smoothness and there should be a reference MEMS surface where both the force should be minimum such a way that total force should be small [10]. This is happening for smooth MEMS surface. Now, adhesional loading force for rough and intermediate MEMS is much more than that of smooth MEMS surface due to mainly Hertzian deformation force. Similarly, adhesional loading force of super smooth MEMS surface is much more than that of smooth MEMS surface due to mainly high adhesive force.

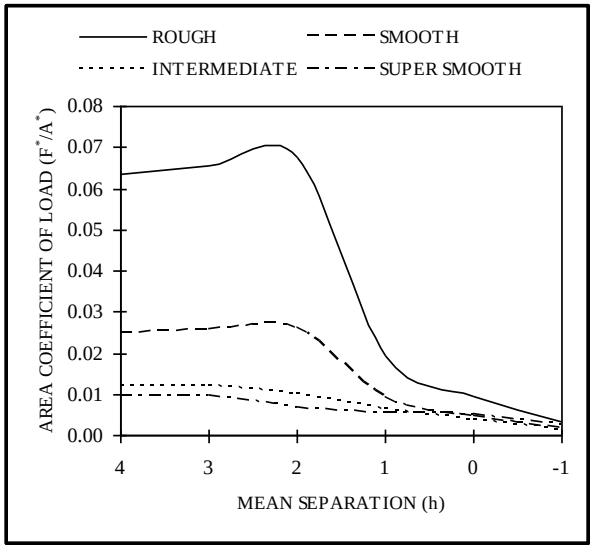


Fig.4 Area coefficient of load

Fig.4 shows area coefficient of load verses dimensionless mean separation. This coefficient is considered to understand the relationship in between real area of contact and loading force. Generally, it is assumed that real area of contact and load are linearly proportional as mentioned by Bowden and Tabor considering plastic deformation of asperity. For mean separation smaller than 1, area coefficient for all four cases are comparatively small and are of the slightly descending with same magnitude. However, as mean separation larger than 2, deviation in the coefficient among the four cases becomes increasing prominent and it maintain almost different constant value with mean separation. The separation in between 2 and 1, there is transition of the coefficient from higher different value to lower descending constant value. So, from the discussion, it is found that it do not support the linear relationship in between real area of contact and the loading force

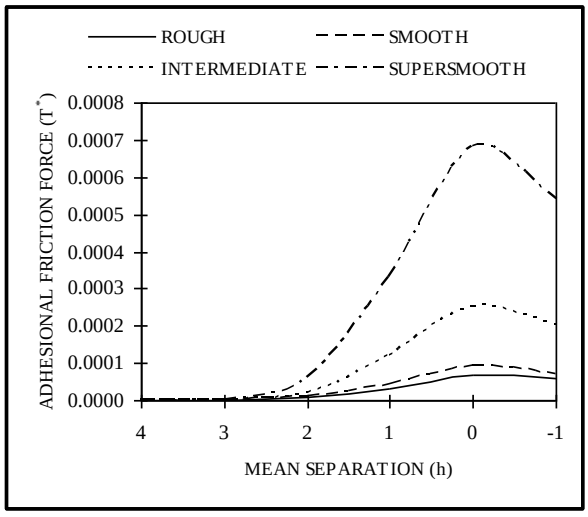


Fig.5 Adhesional friction force

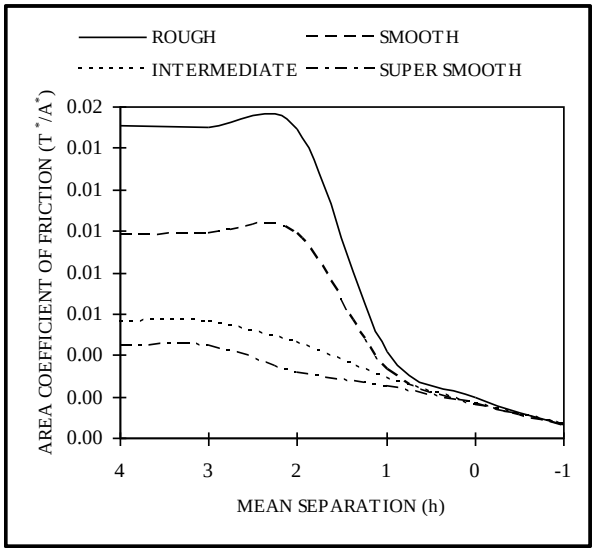


Fig.6 Area coefficient of friction

From Fig.5, adhesional friction force increases with decrement of dimensionless mean separation exponentially. It is found that maximum adhesional friction force for the all MEMS surfaces increases as smoothness of MEMS surface increases. Adhesional friction force for super smooth MEMS surface is very high due to presence of strong attractive adhesive force. On the other hand, adhesional friction force is very small for the rough MEMS surface contact.

Fig.6 shows area coefficient of friction verses dimensionless mean separation and it follows the similar nature of curve as shown for area coefficient of the loading force. Similarly, It shows non linear relationship in between real area of contact and friction force.

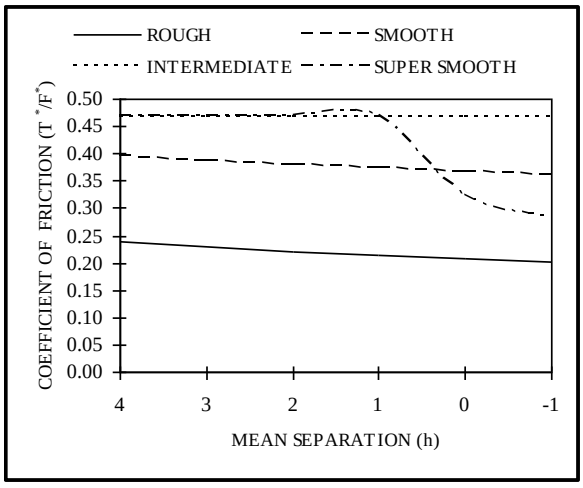


Fig.7 Coefficient of friction

Fig.7 displays variation of coefficient of friction with mean separation. It is found that static coefficient of friction is almost constant except for

the super smooth MEMS surface. So, the Amontons law of static friction is validated for adhesive micromechanical surface contact. Only for the supersmooth MEMS surface contact, coefficient of static friction suddenly drops at close contact though nature of curve of adhesional loading force and adhesional friction force for supersmooth MEMS surface is same.

### 4.2 Investigation on adhesive wear law

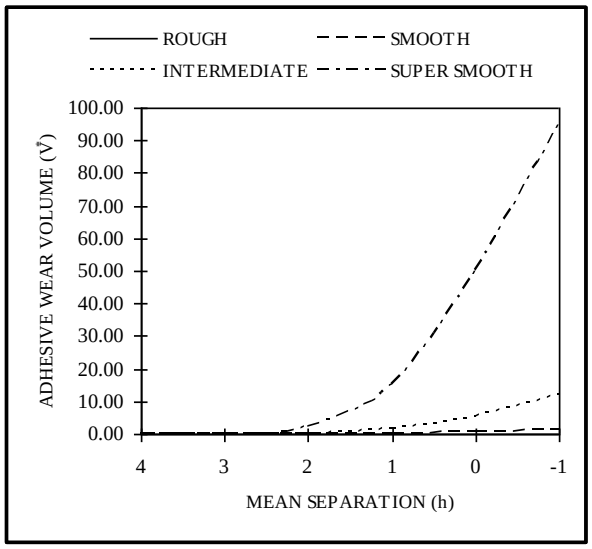


Fig.8 Adhesive wear volume

Fig.8 depicts variation of adhesive wear volume with mean separation. It is found that maximum adhesive wear volume for the all cases of MEMS surfaces increase as smoothness of MEMS surfaces increase. So, super smooth MEMS surface produces maximum adhesive wear volume whereas rough MEMS surface produces very low adhesive wear volume.

Fig.9 shows area coefficient of wear verses dimensionless mean separation. This coefficient is considered to understand the relationship in between real area of contact and wear volume. From the nature of curves, it is found that dimensionless adhesive wear volume is almost linearly proportional with dimensionless real area of contact. So area coefficient of wear is almost constant.

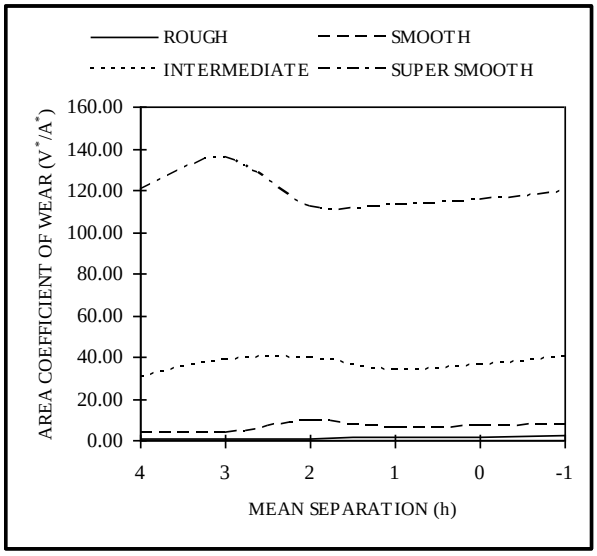


Fig.9 Area coefficient of wear

So, Area coefficient of wear $= \frac{V^*}{A^*} = \frac{V}{A\sigma} = K_{adh}$

$$\Rightarrow V = K_{adh} A\sigma$$

Where real area of surface contact, $A = \frac{P}{H}$ according to Bowden and Tabor theory

$$\Rightarrow V = K_{adh} \frac{P}{H} \sigma$$

Where V= Wear volume, $K_{adh}$ = adhesive wear coefficient (i.e. area coefficient of wear), P = normal load, H = soft material hardness, σ = rms roughness of surface.

According to new adhesive wear law, adhesive wear coefficient increases with increment of MEMS surface contact. And $K_{adh}$ = 0.25 for rough surface, $K_{adh}$ = 5 for smooth surface, $K_{adh}$ = 30 for intermediate surface, and $K_{adh}$ = 120 for super smooth surface.

Now, wear rate, $\dot{V} = v \times$ no. of pass per revolution × RPS

$$= v \times n_p \times RPS$$

Generally, Pin on Disk tester are commonly used to measure wear rate. If circular cross sectional pin of diameter, d is placed on disk at diameter, D,

no. of pass per revolution, $n_p$

$$= \frac{\text{Total area crossed}}{\text{Cross sectional area of pin}} = \frac{\pi Dd}{\pi d^2/4} = 4\frac{D}{d}$$

However, in comparison of new adhesive wear law with Archard's law of adhesive wear, the new law is much more appropriate from the point view of volume concept. In case of well accepted Archard's law of adhesive wear, sliding distance is on the plane of real area of contact and so, how does multiplication of both the two parameter produce volume whereas in case of new law of adhesive wear, r.m.s. roughness perpendicular to the plane of real area of contact which produces volume removal in the form of adhesive wear.

## 5. Conclusions

The study is the theoretical investigation on existing static friction coefficient and adhesive wear law. From the study of micromechanical contact of MEMS surfaces, following conclusions could be drawn:

a) When micro-rough surfaces are come in contact due to application of external force, spherical tip of the contacting asperities form adhesive bond followed by JKR adhesion theory.

b) As smoothness of surfaces increase, it produces much more strong adhesive bond at the tip of the contacting asperities.

c) Real area of contact increases with adhesional loading force nonlinearly which is generally, considered linearly proportional as stated by Bowden and Tabor.

d) Similarly, real area of contact and static adhesional friction force are also nonlinearly proportional.

e) Static coefficient of friction is almost constant for micromechanical surface contact which is theoretical evidence of Amonton's law of friction.

f) Justified new adhesive wear law is developed where adhesive wear volume is equal to multiplication of real area of contact and rms roughness. Coefficient of adhesive wear increases as smoothness of surface increase.

g) Finally, though above study is done for micro-rough surface contact of MEMS but it could be applicable for macroscopic study of tribo-system as interface is always microscopic.

## Acknowledgements

I would humbly thank to Prof. B Halder, NIT Durgapur, India whose inspiration and support have made the work successful.

## References

[1] G Amontons, *Histoire de l'Académie Royale des Sciences avec les Mémoires de Mathématique et de Physique* (1699)

[2] F P Bowden and D Tabor, *The Friction and Lubrication of Solids* (Oxford University Press, New York 1950)

[3] K L Jhonson, K Kendall, and A D Roberts, Surface energy and the contact of elastic solids, *Proc. R. Soc. Lond.,* A 324, 1971, 301-313

[4] B V Derjaguin, V M Muller, and YU P Toporov, Effect of contact deformation on the adhesion of particles, *J. Coll. and Inter. Sc.*, 53, 1975, 314-326

[5] W R Chang, I Etsion, and D B Bogy, Adhesion model for metallic rough surfaces, *Journal of Tribology,* 110, 1988, 50-56

[6] S K Roy Chowdhury and P Ghosh, Adhesion and adhesional friction at the contact between solids, *Wear,* 174, 1994, 9-19

[7] A R Savkoor and G A D Briggs, The effect of tangential force on the contact of elastic solids in adhesion *Proc. R. Soc. Lond.*, A 356, 1977, 103-114

[8] J A Greenwood, and J B P Williamson, Contact of nominally flat surfaces. *Proc. R. Soc. Lond.,* A 295, 1966, 300-319

[9] N Tayebi and A A Polycarpou, Adhesion and contact modeling and experiments in microelectromechanical systems including roughness effects, *Microsyst. Technol.,* 12, 2006, 854-869

[10] B Bera, Adhesion and adhesional friction of micromechanical surface contact. *Journal of Engineering and Applied Sciences,* 6, 2011, 104-108

[11] J F Archard, Contact and rubbing of flat surfaces. *Journal of Applied Physics,* 24, 1953, 981-988

## APPENDIX A

Table.1 Input data

| Combined MEMS Surfaces | Rough | Smooth | Intermidiate | Super Smooth |
|---|---|---|---|---|
| $\eta$ ($m^{-2}$) | $14.7.10^{12}$ | $11.1.\ 10^{12}$ | $17.10^{12}$ | $26.10^{12}$ |
| R (m) | $0.116.10^{-6}$ | $0.45.10^{-6}$ | $1.7.10^{-6}$ | $26.10^{-6}$ |
| $\sigma$ (m) | $15.8.10^{-9}$ | $6.8.10^{-9}$ | $1.4.10^{-9}$ | $0.42.10^{-9}$ |
| $\gamma$ (N/m) | 0.5 | 0.5 | 0.5 | 0.5 |
| K ($N/m^2$) | $112.10^{9}$ | $112.10^{9}$ | $112.10^{9}$ | $112.10^{9}$ |
| G ($N/m^2$) | $18.42.10^{9}$ | $18.42.10^{9}$ | $18.42.10^{9}$ | $18.42.10^{9}$ |
| $A_0$ | $27.10^{-3}$ | $34.10^{-3}$ | $41.10^{-3}$ | $53.10^{-3}$ |
| $B_0$ | $2.825.10^{-4}$ | $6.565.10^{-4}$ | $31.887.10^{-4}$ | $74.405.10^{-4}$ |
| $R_0$ | 7.342 | 66.176 | 1214.285 | 5600.000 |